AAS 16-227

BROAD SEARCH FOR DIRECT TRAJECTORIES FROM EARTH TO DOUBLE-SATELLITE-AIDED CAPTURE AT JUPITER WITH DEEP SPACE MANEUVERS

Alfred E. Lynam*

Double-satellite-aided capture involves gravity assists of two of Jupiter's Galilean moons while a spacecraft is capturing into Jupiter orbit. In this paper, both gravity assists occur before a Jupiter Orbit Insertion (JOI) maneuver that completes the capture. This particular scheme is easier to navigate than other double-satellite-aided captures because there are no flybys after the JOI maneuver that would be adversely affected by the JOI maneuver's stochastic errors. We also find direct interplanetary trajectories from Earth to Jupiter that include a deep space maneuver (DSM). In each double-satellite-aided capture "window", we use an optimizer to find the solution that captures the most mass into Jupiter orbit. The best solutions that launch in either 2022 or 2023 were numerically integrated in GMAT to provide practical double-satellite-aided captures for the Europa Mission's nominal and backup launch windows.

INTRODUCTION

Gravity-assists involve locally hyperbolic flybys of planets or planetary moons that effectively act as ΔV's with regard to the solar or planetary system. Since these effective ΔV's do not require the expenditure of propellant mass, mission designers incorporate them into their trajectories whenever practical. In particular, the Galileo[1,2] and Cassini-Huygens[3,4] missions have performed 32 and more than 150 flybys of Jupiter and Saturn's moons, respectively. In addition to their effective ΔV value as gravity assists, close flybys of planetary moons also allow superb opportunities for scientific observation of these moons.

Before a spacecraft's satellite tour can begin, it must be captured into planetary orbit. Propulsive ΔV's are usually used for capture and are most efficiently performed as orbit insertion maneuvers at the periapsis of the planet-centered hyperbola. Furthermore, the closer the periapsis of the hyperbola is to the planet's surface or atmosphere, the more efficient the insertion maneuver is for capturing the spacecraft. If the planet has sufficiently massive moons, gravity-assists of one or more of the moons may be used to reduce or eliminate the propulsive ΔV needed for capture. These capture sequences are termed "satellite-aided capture"[5−10]

For Saturn orbiters, Titan[11] (with a GM of 8978 km^3/s^2) is the only moon that could provide a practical amount of effective ΔV to assist in a Saturn orbit insertion (SOI) maneuver. However, the extensive rings of Saturn make it difficult to find approach hyperbolas that avoid the rings, flyby Titan, and have an optimal SOI near Saturn's atmosphere. Thus, both the Cassini-Huygens

*Assistant Professor, Mechanical and Aerospace Engineering Department, West Virginia University, ESB, Evansdale Dr. Room 931, Morgantown, WV 26506-6106. Member AIAA. Member AAS.

Table 1. Perijoves and ΔV costs required to capture into a 200-day orbit for unaided capture and single-, double-, triple-, and quadruple-satellite-aided capture sequences.

Perijoves	13 R_J	9 R_J)	5 R_J)	1.01 R_J)
Unaided ΔV	1317 m/s	1101 m/s	825 m/s	371 m/s
Single ΔV	863 m/s	771 m/s	556 m/s	308 m/s
Double ΔV	498 m/s	529 m/s	330 m/s	228 m/s
Triple ΔV	—	330 m/s	202 m/s	190 m/s
Quadruple ΔV	—	—	—	159 m/s

mission[3,4] and the canceled Titan Saturn System mission (TSSM)[12] did not use Titan flybys to reduce the SOI maneuver ΔV. Earth's moon[13] (with a GM of 4902 km^3/s^2) can be useful for satellite-aided capture for low V_∞ Earth return missions,[7] especially for SEP missions. Uranus and Neptune have much smaller moons—Titania[14] has a GM of 228 km^3/s^2 and Triton[15] has a GM of 1428 km^3/s^2—that are not particularly useful for satellite-aided capture.

Satellite-aided capture is by far most effective for Jupiter orbiter missions. Callisto[16] (with a GM of 7179.289 km^3/s^2), Ganymede[17] (with a GM of 9887.834 km^3/s^2), Europa[18] (with a GM of 3202.739 km^3/s^2), and Io[19] (with a GM of 5959.916 km^3/s^2) are all massive enough to provide gravity assists with large equivalent ΔV's. Galileo performed its single-satellite-aided capture using a flyby of Io and a Jupiter orbit insertion (JOI) maneuver.[1,2] Since Jupiter has four large moons, multiple-satellite-aided capture using two, three, or four moons is also possible. Table 1 compares ΔV costs of various types of satellite-aided capture at Jupiter.

Because it is rare for all four Galilean moons to align properly with an interplanetary trajectory from Earth, quadruple-satellite-aided captures occur only once every 10 years.[20] Due to their excessively low perijoves of 1-2 Jupiter radii (R_J) that are deep within Jupiter's radiation environment, they are also considerably less practical than double- or triple-satellite-aided capture.[20] Triple-satellite-aided captures at Jupiter have been studied extensively,[20−28] so their properties are well-understood. Triples are useful both for reducing ΔV costs for chemical missions[25] and for reducing Jupiter capture orbit periods for SEP missions,[26,28] but their main challenge is that they require advanced navigation techniques because they contain three closely spaced flybys and a possible chemical JOI maneuver.[29]

This paper focuses on double-satellite-aided capture at Jupiter, which has also been studied by several authors.[5,6,8,21,22,27,30–33] In particular, Lynam[34] performed a broad-search from 2020 to 2060 for one particular type of double-satellite-aided capture— Callisto-Ganymede-JOI (CGJ) capture. That broad search focused on finding direct ballistic interplanetary trajectories from Earth to Jupiter that capture into Jupiter orbit with CGJ captures. Five promising CGJ solutions were found by the broad search in the 2023 backup launch window for the Europa Mission and integrated in NASA Goddard's General Mission Analysis Tool (GMAT). However, Lynam found no CGJ solutions in the 2022 nominal launch window.

This paper builds on Lynam's[34] work by investigating three different double-satellite-aided capture sequences: Callisto-Ganymede-JOI (CGJ), Ganymede-Europa-JOI (GEJ), and Ganymede-Io-JOI (GEJ). These sequences were chosen because they are easier to navigate than double-satellite-aided capture sequences such as Callisto-JOI-Ganymede (CJG) or Ganymede-JOI-Io (GJI) because

their JOI maneuvers occur after both flybys. The broad search in this paper also allows deep space maneuvers (DSM) in between Earth and Jupiter, which enables a broader range of solutions than the ballistic interplanetary trajectories found by Lynam. In order to narrow down the solution space, only the trajectory with the maximum post-JOI mass is recorded for each double-satellite-aided capture window. The post-JOI mass is found by assuming a SLS Block I launch vehicle and a bipropellant main engine with an Isp of 325s for the DSM and JOI maneuvers. We also find two dozen GMAT solutions in the 2022 and 2023 launch windows that have DSM ΔV's, JOI ΔV's, and Earth launches. Some of the trajectories in this paper are analyzed from a statistical ΔV and navigation perspective by Lynam and Didion.[35]

METHODOLOGY

Patched Conic Model and Phase Angles

This paper uses the same methodology as Lynam[34] in finding double-satellite-aided capture trajectories, but it will be described briefly for completeness. The angle between a set of Galilean moons (or between a Galilean moon and the Sun) at a given time is called a "phase angle" (see Fig. 1 for a geometric definition). Using a circular, coplanar patched-conic model, we find the phase angle ranges that are consistent with double-satellite-aided capture sequences that could possibly arrive at Jupiter on an efficient interplanetary trajectory from Earth. For the CGJ captures that were found by Lynam, the relevant phase angles were the Callisto-Ganymede ($\Delta\lambda_{\text{Ca,Ga}}$) and Callisto-Sun ($\Delta\lambda_{\text{Ca,Sun}}$) phase angles. This paper also uses the same phase angles for CGJ captures, but uses different phase angles for GEJ and GIJ captures. GEJ captures use the Ganymede-Europa ($\Delta\lambda_{\text{Ga,Eu}}$) and Ganymede-Sun ($\Delta\lambda_{\text{Ga,Sun}}$) phase angles; GIJ captures use Ganymede-Io ($\Delta\lambda_{\text{Ga,Io}}$) and Ganymede-Sun ($\Delta\lambda_{\text{Ga,Sun}}$) phase angles.

For each double-satellite-aided capture sequence, both relevant phase angles have to be within a certain range. The ephemerides of the Galilean moons are searched to find the times when both phase angles are within the correct range. This process reduces the effective size of the search space (and therefore the required computation time for this part of the problem) by more than 99%, while retaining only plausibly feasible solutions. The double flyby solutions feasible times ranges are discretized in terms of two of the orbital elements of the incoming Jupiter-centered asymptote—the V_∞ is varied from 5.1 km/s to 6.3 km/s and the perijove is varied differently for the different double flyby sequences. (We not that this is the perijove of the Jupiter-centered hyperbola before the flybys, the real perijove is always lower than this.) For the CGJ sequences, the incoming perijove ranges from 6.4 R_{J} to 15 R_{J}. For the GEJ sequences, the incoming perijove ranges from 6.0 R_{J} to 9.8 R_{J}. For the GIJ sequences, the incoming perijove ranges from 3.6 R_{J} to 6.3 R_{J}.

For each of the double flyby solutions, the ephemeris time of the first flyby is calculated using the phase angles, and the time of flight is computed based on the patched-conic solutions associated with that phase angle. The ephemeris time of the second flyby is found by adding the first flyby ephemeris time to the time of flight. The ephemerides of the appropriate moons are read to find their position and velocity vectors at the time of their flybys. A Lambert solver is used to solve for the 3D patched-conic solutions for the spacecraft trajectories. The MATLAB Lambert solver was written by Rody Oldenhuis and is available online. The Lambert solver is based on an unpublished experimental Lambert solver by Dario Izzo and a robust Lancaster-Blanchard-Gooding Lambert solver.[36,37] The Lambert solver was compiled in order to speed up program execution since Lambert solutions are needed for an entire array of Callisto and Ganymede positions for each of the many feasible windows.

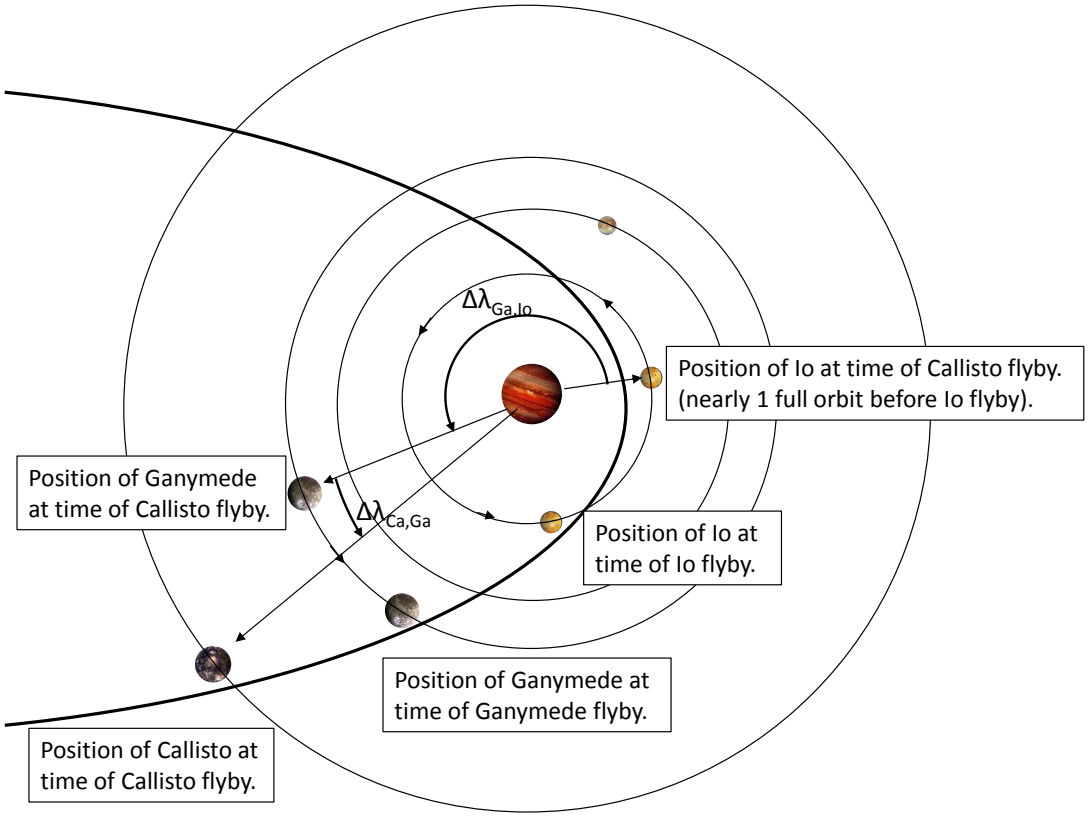

Figure 1. A geometric definition of the Callisto-Ganymede phase angle for a Callisto-Ganymede-JOI (CGJ) double flyby.

The process produces outgoing V_∞ vectors at the first flyby and incoming V_∞ vectors at the second flyby for each of the trajectory solutions within each feasible window from 2020 to 2060. The outgoing V_∞ vectors at the first flyby can be used to model the gravity assist in reverse via the B-plane methodology described by Lynam[34] in Eqs. 9–13. This reversed gravity assist produces the incoming V_∞ vectors for the first flyby (assuming an equatorial flyby). Gauss's f and g functions are used to backward propagate from the incoming V_∞ vectors to Jupiter's sphere of influence. Similarly, the incoming V_∞ vectors at the second flyby can be used to model an equatorial gravity assist that produces the optimal outgoing V_∞ vector for Jovicentric orbital energy reduction. f and g functions are also used to propagate to the perijove of the trajectory, and the JOI ΔV required to capture into a 200-day orbit is calculated. In summary, each double flyby window contains a number of valid incoming Jupiter-centered V_∞ and perijove pairs that are used to solve for ephemeris patched-conic double-satellite-aided capture sequences with JOI ΔV's and backward-propagated Jovicentric states at Jupiter's sphere of influence.

Deep Space Maneuver Optimization

For the interplanetary part of the trajectory, the Jovicentric states at Jupiter's sphere of influence are converted to heliocentric states via Jupiter's ephemeris at that time. Since the incoming Jupiter-centered V_∞ and perijove pairs form a grid of heliocentric states, a grid optimization method is used to find the pair that has the maximum post-JOI mass. MATLAB's fmincon function is used to optimize the deep space maneuver location and the Earth launch time for each pair. Once the best pair is found, a second fine optimization problem is set up that looks for the best solution in the neighborhood of the grid optimal solution. This second optimization problem varies five different parameters: Earth launch time, deep space maneuver location, first flyby B-plane angle, incoming Jupiter-centered V_∞, and incoming perijove. The best solution after the second optimization is usually slightly better than the grid optimal solution. The following describes the "inside" of the optimization function that calculates the final post-JOI mass for each set of five input parameters.

As described above, the heliocentric state is a rather indirect function of the incoming Jupiter-centered V_∞, perijove, and first flyby B-plane.

$$\vec{R}_{\text{helio}} = \vec{R}_{\text{helio}}\left(V_{\infty,\text{Jup}}, R_\text{p}, \theta_1\right) \tag{1}$$

$$\vec{V}_{\text{helio}} = \vec{V}_{\text{helio}}\left(V_{\infty,\text{Jup}}, R_\text{p}, \theta_1\right) \tag{2}$$

where $\vec{R}_{\text{helio}}$ and $\vec{V}_{\text{helio}}$ are the heliocentric position and velocity vectors at Jupiter's sphere of influence, $V_{\infty,\text{Jup}}$ is the incoming Jupiter-centered V_∞, θ_1 is the B-plane angle of the first flyby of the double-satellite-aided capture, and R_p is what the perijove would be if there were no flybys.

For simplicity, the location of the deep space maneuver (DSM) is input in terms of the (negative) change in eccentric anomaly (ΔE) from Jupiter's sphere of influence to that location.

$$E_{\text{DSM}} = E_{\text{helio}}\left(\vec{R}_{\text{helio}}, \vec{V}_{\text{helio}}\right) + \Delta E \tag{3}$$

where E_{DSM} is the heliocentric eccentric anomaly of the DSM location and E_{helio} is the heliocentric eccentric anomaly of the spacecraft at Jupiter's sphere of influence (which is a function of the heliocentric state there). Heliocentric f and g functions are then used to backward propagate to the heliocentric state immediately after the maneuver.

$$\vec{R}_{\text{DSM}} = f_{\text{DSM}}\vec{R}_{\text{helio}} + g_{\text{DSM}}\vec{V}_{\text{helio}} \tag{4}$$

$$\vec{V}^{+}_{\text{DSM}} = \dot{f}_{\text{DSM}}\vec{R}_{\text{helio}} + \dot{g}_{\text{DSM}}\vec{V}_{\text{helio}} \tag{5}$$

where $\vec{R}_{\text{DSM}}$ and $\vec{V}^{+}_{\text{DSM}}$ are the heliocentric position and velocity vectors of the spacecraft immediately after the DSM and the f and g functions are calculated from the heliocentric orbital elements and the eccentric anomalies at Jupiter's sphere of influence and at the DSM location.

The position ($\vec{R}_{\text{Earth}}$) and velocity ($\vec{V}_{\text{Earth}}$) vectors of Earth at the input launch time (t_{Earth}) are extracted from the ephemeris. The Lambert solver is applied again to find the pre-DSM velocity vector ($\vec{V}^{-}_{\text{DSM}}$) and the launch velocity vector ($\vec{V}_{\text{launch}}$). The ΔV_{DSM} and the launch C_3 are found as follows:

$$\Delta V_{\text{DSM}} = \left\| \vec{V}^{+}_{\text{DSM}} - \vec{V}^{-}_{\text{DSM}} \right\| \tag{6}$$

$$C_3 = \left\| \vec{V}_{\text{launch}} - \vec{V}_{\text{Earth}} \right\|^2 \tag{7}$$

The ΔV_{JOI} is an indirect function of the incoming Jupiter-centered V_∞ and perijove.

$$\Delta V_{\text{JOI}} = \Delta V_{\text{JOI}} \left(V_{\infty,\text{Jup}}, R_{\text{p}} \right) \tag{8}$$

A launch curve for the SLS Block I rocket was developed from a logarithmic curve fit of Donahue and Sauvageau's[38] data.

$$m_{\text{launch}} = -7466.331378 \ln C_3 + 37616.827491 \tag{9}$$

where m_{launch} is the launch mass in kg for a given C_3 value in km/s. The spacecraft's main engine is assumed to have an Isp of 325s, so the rocket equation is used to appropriately decrement the mass for the DSM and JOI maneuvers. Thus, the post-JOI mass is a function of the ΔV's and launch C_3:

$$m_{\text{post-JOI}} = m_{\text{post-JOI}} \left(C_3, \Delta V_{\text{DSM}}, \Delta V_{\text{JOI}} \right) \tag{10}$$

where $m_{\text{post-JOI}}$ is the post-JOI mass that is maximized by fmincon by adjusting the five inputs: $V_{\infty,\text{Jup}}$, R_{p}, θ_1, ΔE, and t_{Earth}.

GMAT Trajectories

Integrated trajectories were found in GMAT[39] for the 2022 and 2023 Europa Mission launch windows. The results of the broad search were used to generate initial guesses for the GMAT trajectories. Similarly to Lynam,[34] we use four orbital parameters to target the four B-plane parameters that describe the two flybys. The particular parameters were epoch, inclination, right ascension of the ascending node (RAAN), and argument of perijove of the Jupiter-centered asymptote a few days before the flybys. After the correct parameters were found, the trajectory was backward propagated to either the DSM time from the broad search results or 100-200 days before the double flyby (depending on which is more optimal in the high-fidelity model). The three components of the DSM

ΔV were used to backward target Earth's two B-plane parameters (which would correspond to a low-fidelity Earth launch).

A one-parameter optimization was performed by manually varying the semi-major axis and re-converging the GMAT trajectory. Sometimes this manual variation increased the post-JOI mass from the GMAT results by hundreds of kilograms, but sometimes it only increased it by less than 10 kilograms. The mass results would have been better if all 5 of the parameters could have been varied in GMAT as well as MATLAB, but the base amount of time to converge a GMAT trajectory was too high. Furthermore, the 4 to 4 targeter was somewhat unstable, so manual intervention was sometimes needed to ensure that the trajectories converged. We also emphasized breadth of GMAT solutions rather than concentrating on any one solution.

RESULTS

The broad searches for CGJ, GEJ, and GIJ double-satellite-aided captures from 2020-2060 were completed using MATLAB. The CGJ search took 17 hours to complete on a desktop PC with 2 Intel Xeon CPU E5-2687W @ 3.10 GHz processors. The GEJ and GIJ searches took 13 and 20 hours, respectively. Although a substantial amount of other data was collected in these broad searches, for (relative) brevity purposes only the launch times, post-JOI masses, and perijoves are summarized in Figs. 2–7. The CGJ, GEJ, and GIJ results are listed in separate subsections below. As a point of comparison, the post-JOI mass of the nominal GJ Europa mission[40] is 3420 kg using the same assumptions (the interpolated SLS Block I launch curve and an Isp of 325 s).

Broad Search CGJ Results

As depicted in Fig. 2, the CGJ results had a wide range of perijove values and a wide range of post-JOI masses. The minimum values for the perijoves and masses were artificially chosen to be 5 R_{J} and 3000 kg, respectively. These decisions are due to the fact that GIJ sequences are much better and more available than CGJ sequences at the lower perijoves and that a post-JOI mass below 3000 kg would be substantially worse than even the Ganymede-JOI single-satellite-aided capture sequence that is being investigated for the nominal Europa mission.[40] The results show that launch windows with several good trajectories occur about once every three years. Similarly to the results of Lynam,[34] there are no good solutions in the nominal 2022 launch window,[40] but there are several good solutions in the backup 2023 launch window. Figure 3 is a zoomed in view of the CGJ trajectories that launch in July 2023.

In the top half of Fig. 3, we note that most of the trajectories in this window have post-JOI masses above 3800 kg. Since all the trajectories launch in the same launch window and the abscissa of the figure is the time of flight, we also note that the Jupiter arrival times of the trajectories are separated by intervals of 50 days. This is due to the peculiarity of the 3:7 near-resonance between Callisto and Ganymede,[41] which has a 50 day repeat period in inertial space. In the bottom half of Fig. 3, the perijoves of each of these trajectories are plotted. We note that the perijoves for this launch window do increase monotonically with increasing time of flight, however, the best in the group has a perijove of slightly under 9 R_{J}. While 13 R_{J} and 9 R_{J} CGJ's have very similar performance in terms of ΔV (567 m/s vs. 558 m/s), Jupiter's radiation environment is several times less severe at 13 R_{J} than it is at 9 R_{J}. Thus, it would have been more ideal if a 13 R_{J} CGJ had been available in the 2023 launch window.

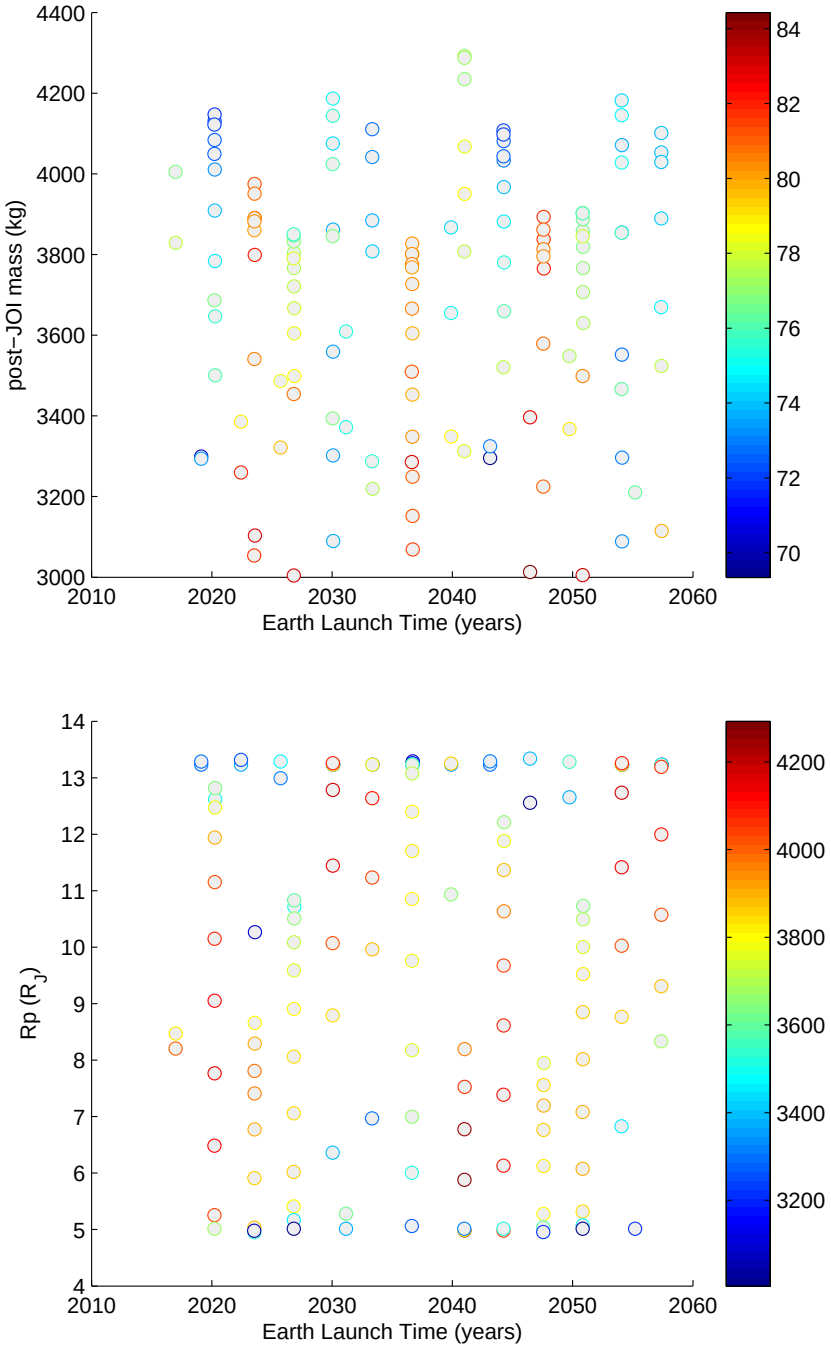

Figure 2. Post-JOI masses (top) and perijoves (bottom) for trajectories from Earth to CGJ capture at Jupiter. Colorbar on top figure represents Earth launch C_3 in km^2/s^2; colorbar on bottom figure represents post-JOI mass in kgs.

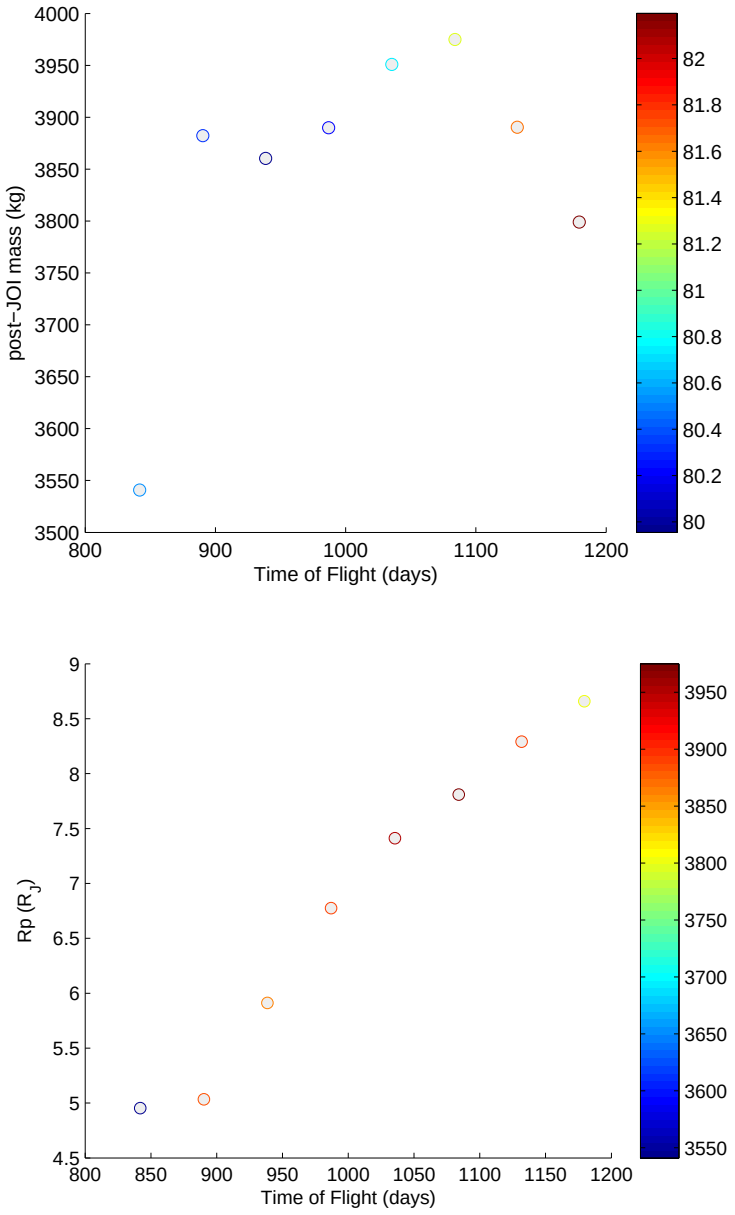

Figure 3. A zoomed in view of CGJ captures in the July 2023 launch window. Post-JOI masses (top) and perijoves (bottom) for trajectories from Earth to CGJ capture at Jupiter. Since the launch dates are nearly identical, the times of flight in days are on the abscissa instead; these correspond to Jupiter arrivals from Nov. 2025 to Oct. 2026. Colorbar on top figure represents Earth launch C_3 in km^2/s^2; colorbar on bottom figure represents post-JOI mass in kgs.

Table 2. GMAT double-satellite-aided capture solutions for the June 2022 launch window.

Solution	Launch	Launch C_3	Arrival	$m_{\text{post-JOI}}$	Perijove
GIJ 1	6/22/2022	84.0 km^2/s^2	1/20/2025	3958 kg	5.44 R_{J}
GIJ 2	6/23/2022	84.4 km^2/s^2	1/27/2025	3968 kg	4.55 R_{J}
GIJ 3	6/23/2022	84.4 km^2/s^2	2/3/2025	3954 kg	3.69 R_{J}
GIJ 4	6/19/2022	82.6 km^2/s^2	2/10/2025	3781 kg	3.24 R_{J}
GIJ 5	6/29/2022	85.1 km^2/s^2	7/3/2025	3570 kg	5.61 R_{J}
GIJ 6	6/30/2022	85.3 km^2/s^2	7/10/2025	3836 kg	4.87 R_{J}
GEJ 1	6/22/2022	83.4 km^2/s^2	4/9/2025	3274 kg	8.69 R_{J}
GEJ 2	6/21/2022	83.4 km^2/s^2	4/16/2025	3200 kg	7.30 R_{J}

Broad Search GEJ Results

The results for the GEJ broad search are plotted in Fig. 4. The results indicate that there are optimal GEJ solutions about once every 12 years, which is approximately Jupiter's orbital period around the Sun. (It would be interesting to investigate mathematical and physical reasons for this correlation, but that is beyond the scope of this paper.) There are less optimal GEJ trajectories available on an approximately yearly basis. Unfortunately, the GEJ solutions that launch in 2022 and 2023 are rather suboptimal. In the top half of Fig. 5, the post-JOI mass values for two of the 2022 launches are on the left side of the figure and are slightly better than the three 2023 launches on the right side of the figure. (We note that there are two other 2022 launches in Fig. 4, but they are worse than the 2023 launches.) These GEJ results are comparable in post-JOI mass to a Ganymede-JOI capture like that of the nominal Europa mission,[40] so they are not particularly useful.

Broad Search GIJ Results

As shown in Fig. 6, the results for the GIJ captures were clearly the best. There are optimal GIJ capture trajectories available for every synodic period between Earth and Jupiter. We note that there is a 12-year repeat pattern similar to that of the GEJ captures. In the case of the GIJ captures, however, the best years have post-JOI masses of more than 4500 kg and the worst years have post-JOI masses of around 4000 kg. The perijoves of GIJ captures are required to be less than Io's perijove of 5.9 R_{J}, but there are always GIJ captures available that have good mass properties and are only slightly below Io's orbit. Fig. 7 shows that there are excellent GIJ captures available for both the June 2022 and the July 2023 launch windows.

GMAT Results

The 2022 and 2023 results from the broad search that were plotted in Figs. 3, 5, and 7 were used as initial guesses for integrated, high-fidelity GMAT trajectories. The GMAT trajectory results for 2022 and 2023 are in Tables 2 and 3, respectively. There are no CGJ solutions in 2022, so only the GIJ and GEJ solutions are included in Table 2. Table 3 does not include GEJ solutions because the CGJ solutions available in the 2023 launch window are much better than the GEJ solutions in terms of both perijove and post-JOI mass.

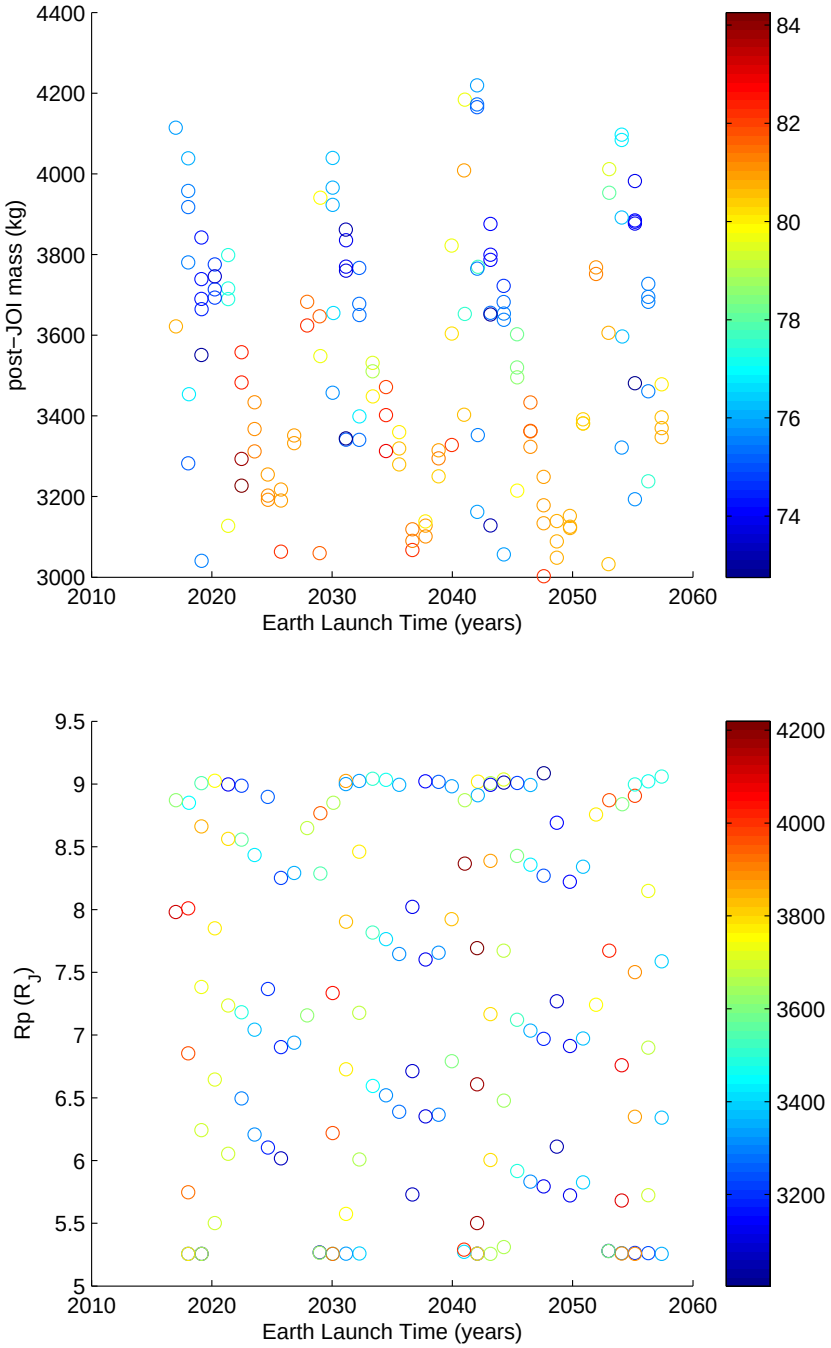

Figure 4. Post-JOI masses (top) and perijoves (bottom) for trajectories from Earth to GEJ capture at Jupiter. Colorbar on top figure represents Earth launch C_3 in km^2/s^2; colorbar on bottom figure represents post-JOI mass in kgs.

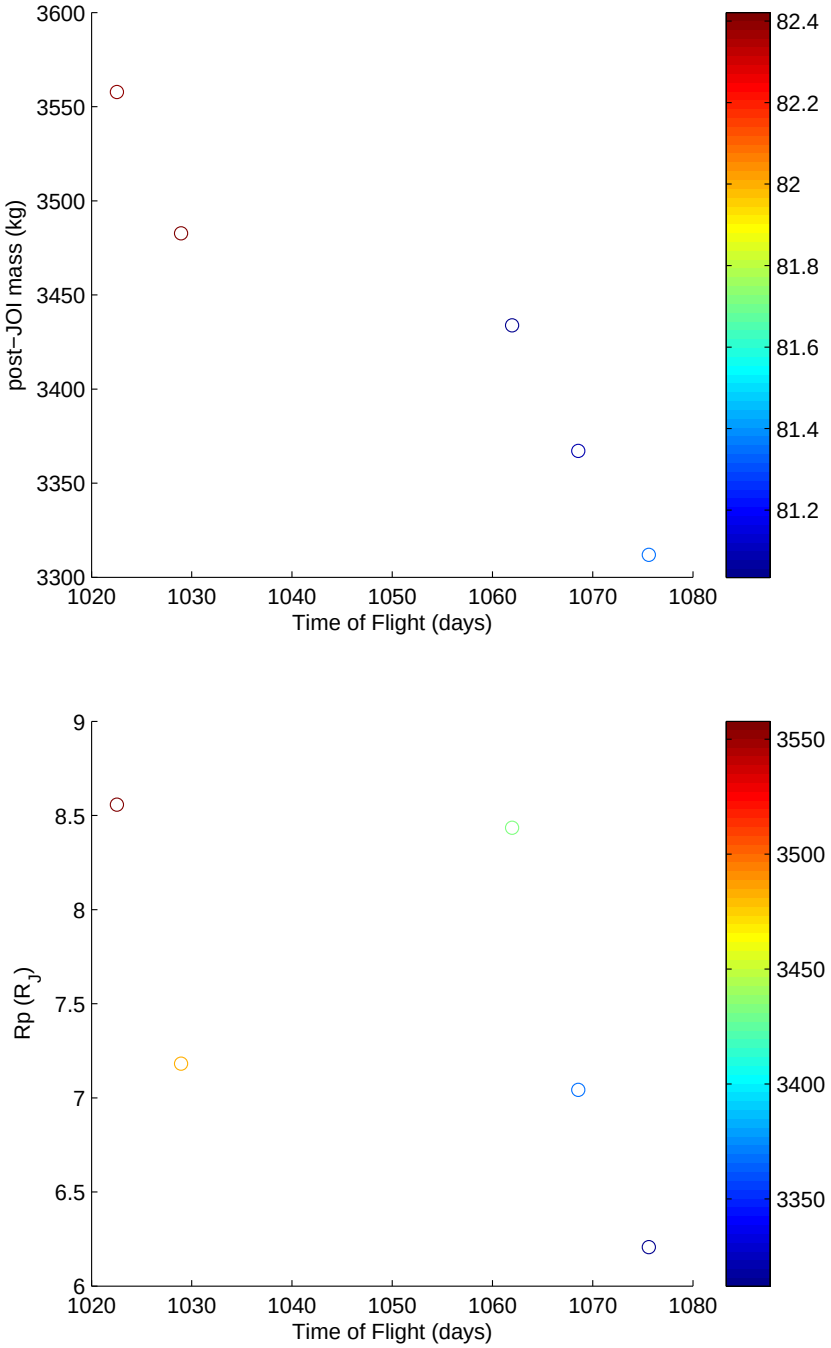

Figure 5. A zoomed in view of GEJ captures in the June 2022 (two on left) and July 2023 (three on right) launch windows. Post-JOI masses (top) and perijoves (bottom) for trajectories from Earth to GEJ capture at Jupiter. Colorbar on top figure represents Earth launch C_3 in km^2/s^2; colorbar on bottom figure represents post-JOI mass in kgs.

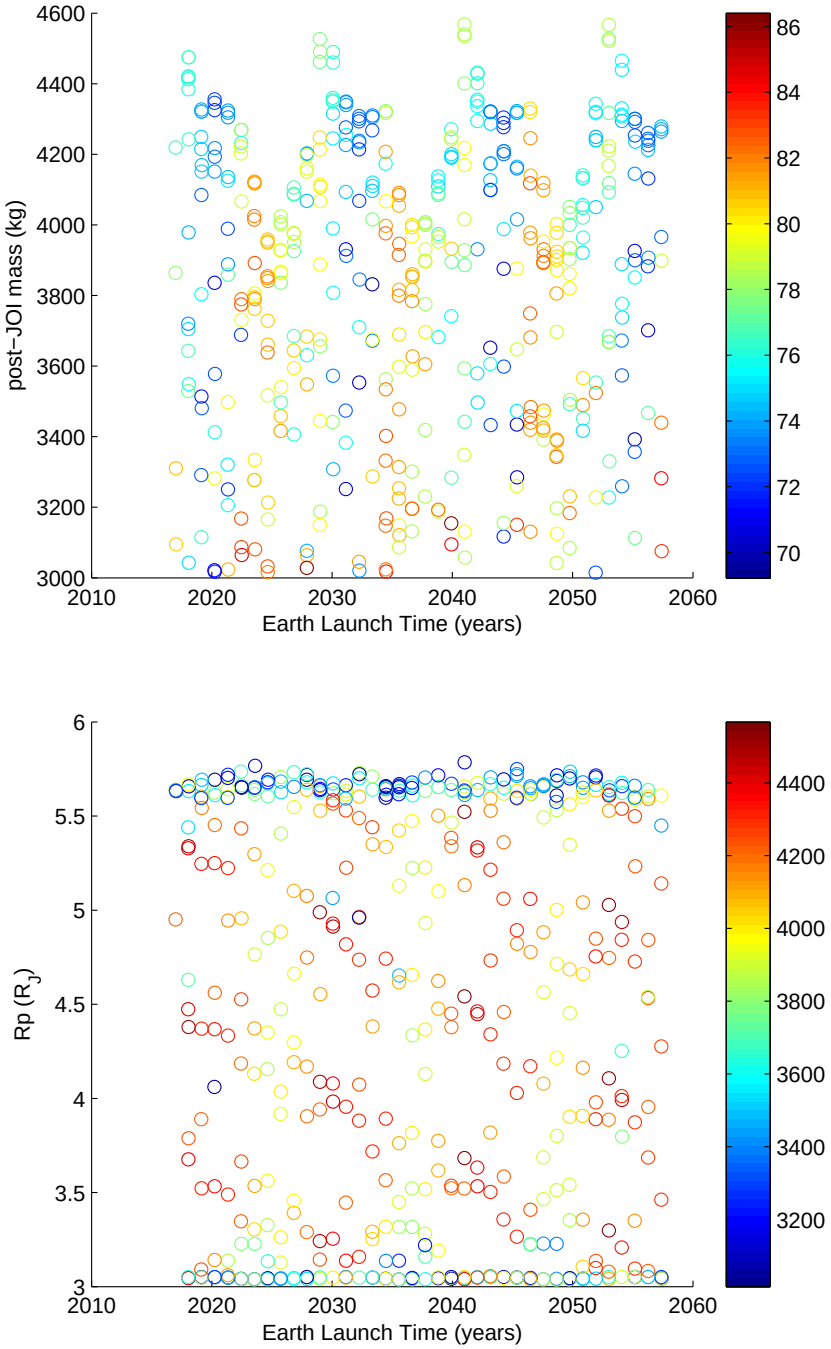

Figure 6. Post-JOI masses (top) and perijoves (bottom) for trajectories from Earth to GIJ capture at Jupiter. Colorbar on top figure represents Earth launch C_3 in km^2/s^2; colorbar on bottom figure represents post-JOI mass in kgs.

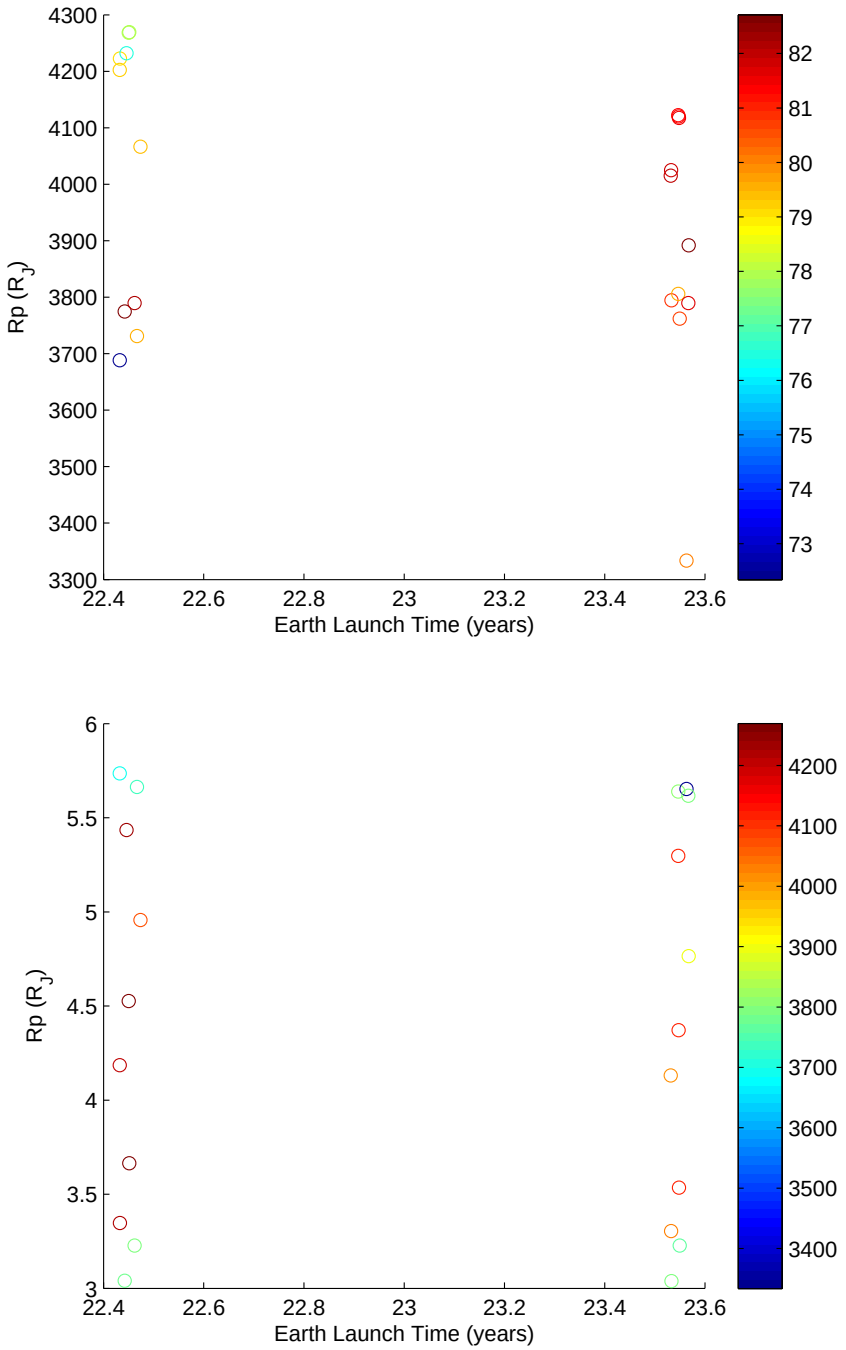

Figure 7. A zoomed in view of GIJ captures in the June 2022 and July 2023 launch windows. Post-JOI masses (top) and perijoves (bottom) for trajectories from Earth to GIJ capture at Jupiter. Colorbar on top figure represents Earth launch C_3 in km^2/s^2; colorbar on bottom figure represents post-JOI mass in kgs.

Table 3. GMAT double-satellite-aided capture solutions for the July 2023 launch window.

Solution	Launch	Launch C_3	Arrival	$m_{\text{post-JOI}}$	Perijove
GIJ 7	7/12/2023	82.2 km^2/s^2	10/19/2025	3803 kg	4.20 R_J
GIJ 8	7/12/2023	82.7 km^2/s^2	10/26/2025	3824 kg	3.39 R_J
GIJ 9	7/13/2023	81.0 km^2/s^2	11/2/2025	3759 kg	3.03 R_J
GIJ 10	7/16/2023	81.4 km^2/s^2	3/26/2026	3704 kg	5.64 R_J
GIJ 11	7/19/2023	81.5 km^2/s^2	4/3/2026	4027 kg	5.31 R_J
GIJ 12	7/16/2023	83.7 km^2/s^2	4/9/2026	4002 kg	4.42 R_J
GIJ 13	7/17/2023	83.8 km^2/s^2	4/16/2026	3980 kg	3.58 R_J
GIJ 14	7/22/2023	80.8 km^2/s^2	4/23/2026	3774 kg	3.19 R_J
CGJ 1	7/16/2023	80.6 km^2/s^2	12/22/2025	3778 kg	5.12 R_J
CGJ 2	7/18/2023	80.3 km^2/s^2	2/10/2026	3808 kg	6.08 R_J
CGJ 3	7/22/2023	80.5 km^2/s^2	3/30/2026	3802 kg	6.86 R_J
CGJ 4	7/22/2023	81.2 km^2/s^2	5/21/2026	3850 kg	7.40 R_J
CGJ 5	7/23/2023	82.0 km^2/s^2	7/10/2026	3857 kg	7.77 R_J
CGJ 6	7/25/2023	82.5 km^2/s^2	8/30/2026	3766 kg	8.22 R_J
CGJ 7	7/27/2023	83.2 km^2/s^2	10/19/2026	3669 kg	8.57 R_J

DISCUSSION

Since the GMAT results used the broad search results as initial guesses, they can be directly compared with each other. The GMAT GIJ results in the 2022 launch window were usually between 100 and 300 kg worse than the broad search results; the exception was GIJ 4, which was only 9 kg worse (3781 vs 3790 kg). The GMAT GIJ results from the 2023 launch window were usually between 100 kg and 200 kg worse than the broad search results. The two exceptions were GIJ 9, which was only 36 kg worse (3759 kg vs 3795 kg), and GIJ 14, which was 12 kg better (3774 kg vs 3762 kg). The 2 GMAT GEJ results were about 300 kg worse than their corresponding broad search results. Since the broad search results were already bad, it would be much better to use the nominal GJ capture[40] (3420 kg) than to use the GMAT 2022 GEJ captures (3274 kg and 3200 kg) for the Europa mission. The GMAT CGJ results were about 100 kg worse than the broad search CGJ results.

The GMAT results were likely worse than the broad search results because they only had one parameter optimized manually (semi-major axis of the incoming Jupiter-centered hyperbola), while the broad search results had 5 optimization parameters. If better optimization strategies and software were used, it is likely that the high-fidelity results would approximately match the broad search results. The GMAT results were close enough to the broad search results to provide proof of concept for the broad search methodology, and most of them had better post-JOI mass properties than the nominal GJ capture even though they were suboptimal.

The primary disadvantage of all the double-satellite-aided capture results versus the nominal GJ capture is that their perijoves are all substantially lower. The CGJ result with the highest perijove was CGJ 7 with a perijove of 8.57 R_J. The GEJ result with the highest perijove was GEJ 1 with a perijove of 8.69 R_J (although its mass results were bad). The GIJ result with the highest perijove was GIJ 10 with a perijove of 5.64 R_J. These can be compared with the nominal GJ capture that

had a perijove of around 12 R_J.[40]

The reason the lower perijoves are worse than the higher perijoves are that the spacecraft would be exposed to additional radiation and that it would have to expend more perijove raise maneuver (PJR) ΔV to avoid the radiation on subsequent orbits. Since the double-satellite-aided capture allows substantial propellant mass savings, it is possible that some of those savings could be used to increase the radiation shielding mass. A full trade study of post-JOI mass vs. initial perijove, PJR propellant mass, and radiation shielding mass would be interesting but is beyond the scope of this paper.

In spite of their radiation disadvantages, the GIJ captures are generally the most promising double-satellite-aided capture sequences because many of them are available in both launch windows and because they have the best post-JOI mass performance. Rather than using an expensive PJR to increase their subsequent perijoves to 12 R_J or higher, Io could be used to pump down the orbital period rather than Ganymede and then flybys of Callisto could be used to raise the perijove later. This strategy is essentially the same as that proposed by Kloster et al.[42] for the 2008 Jupiter Europa Orbiter mission study. While this strategy would increase the radiation exposure of the spacecraft, it would also substantially increase the spacecraft's usable mass and possibly enable a small Europa lander to be included with the mission.

The CGJ and GEJ captures in the 2022 and 2023 launch windows are underperforming compared to those in subsequent launch windows. While the CGJ's available in 2023 would be better than the nominal GJ, the margin of superiority of the CGJ's in other windows would be greater since other windows have CGJ's with perijoves similar to the nominal GJ but much better post-JOI masses. As noted earlier, the GEJ's in the 2022 and 2023 launch windows are worse than the nominal GJ. Other launch windows have GEJ's that would be better than the nominal GJ in terms of post-JOI mass, but their perijoves would always be worse because Europa is deeper in Jupiter's radiation environment than Ganymede.

CONCLUSIONS

The patched-conic, broad search algorithm successfully found the best CGJ, GEJ, and GIJ double-satellite-aided capture solutions with optimal DSM's for each launch window from 2020 to 2060. Optimal GIJ captures with high post-JOI masses were available in every launch window, while optimal GEJ and CGJ solutions were somewhat less common. The GEJ and CGJ solutions did have better perijoves (therefore less radiation exposure) than the GIJ captures, however. The 2022 and 2023 launch windows were investigated in detail and integrated GMAT trajectories were found for many of the more promising patched-conic solutions. Excellent GIJ solutions were found for both launch windows, no good GEJ solutions were found for either launch window, and good CGJ solutions were found for the 2023 launch window. The GIJ and CGJ solutions had far better mass properties than the nominal GJ single-satellite-aided capture solution for the Europa mission, albeit with lower perijoves and more radiation exposure.

REFERENCES

[1] C. Potts and M. Wilson, "Maneuver Design for the Galileo VEEGA Trajectory," *AAS Paper 93-566, Proceedings of the AAS/AIAA Astrodynamics Specialist Conference*, Victoria, B.C., Canada, Aug. 1993.

[2] T. Barber, F. Krug, and B. Froidevaux, "Initial Galileo Propulsion System In-Flight Characterization," *AIAA Paper No: 93-2117, Proceedings of the AIAA/SAE/ASME/ASEE 29th Joint Propulsion Conference and Exhibit*, Monterrey, CA, June 1993.

[3] T. D. Goodson, D. L. Gray, Y. Hahn, and F. Peralta, "Cassini Maneuver Experience: Finishing Inner Cruise," *AAS Paper 00-167, Proceedings of the AAS/AIAA Spaceflight Mechanics Meeting*, Clearwater, FL, January 2000.

[4] D. Roth, P. Antreasian, J. Bordi, K. Criddle, R. Ionasescu, R. Jacobson, J. Jones, M. C. Meed, I. Roundhill, and J. Stauch, "Cassini Orbit Reconstruction from Jupiter to Saturn," *AAS Paper 05-311, Proceedings of the AAS/AIAA Astrodynamics Specialist Conference*, Lake Tahoe, CA, August 2005.

[5] R. W. Longman, "Gravity Assist from Jupiter's Moons for Jupiter-Orbiting Space Missions," tech. rep., The RAND Corp., Santa Monica, CA, 1968.

[6] R. W. Longman and A. M. Schneider, "Use of Jupiter's Moons for Gravity Assist," *Journal of Spacecraft and Rockets*, Vol. 7, No. 5, May 1970, pp. 570–576.

[7] J. K. Cline, "Satellite Aided Capture," *Celestial Mechanics*, Vol. 19, May 1979, pp. 405–415.

[8] K. T. Nock and C. Uphoff, "Satellite Aided Orbit Capture," *AAS Paper 79-165, Proceedings of the AAS/AIAA Astrodynamics Specialist Conference*, Provincetown, MA, June 25–27, 1979.

[9] M. Malcolm and C. McInnes, "Spacecraft Planetary Capture Using Gravity-Assist Maneuvers," *Journal of Guidance, Control, and Dynamics*, Vol. 28, March-April 2005, pp. 365–368.

[10] C. H. Yam, *Design of Missions to the Outer Planets and Optimization of Low-Thrust, Gravity-Assist Trajectories via Reduced Parameterization*. PhD thesis, School of Aeronautics and Astronautics, Purdue University, West Lafayette, IN, May 2008, pp. 96–104.

[11] R. A. Jacobson, P. G. Antreasian, S. Ardalan, K. E. Criddle, R. Ionasescu, J. B. Jones, D. Parcher, F. J. Pelletier, D. C. Roth, P. Thompson, and A. Vaughan, "The Gravity Field of the Saturnian System and the Orbits of the Major Saturnian satellites," *Saturn After Cassini-Huygens Symposium*, Imperial College, London, UK, 2008.

[12] N. J. Strange, T. R. Spilker, D. F. Landau, T. Lam, D. Lyons, and J. Guzman, "Mission Design for the Titan Saturn System Mission Concept," *AAS Paper 09-356, AAS/AIAA Astrodynamics Conference*, Pittsburgh, PA, August 2009.

[13] E. M. Standish, "JPL Planetary and Lunar Ephemerides, DE405/LE405," tech. rep., Jet Propulsion Laboratory, Pasadena, CA, 1998.

[14] R. A. Jacobson, "The Gravity Field of the Uranian System and the Orbits of the Uranian Satellites and Rings," *BAAS*, Vol. 39, 2007.

[15] P. C. Thomas, "The Shape of Triton from Limb Profiles," *Icarus*, Vol. 148, 2000.

[16] J. D. Anderson, R. A. Jacobson, T. P. McElrath, W. B. Moore, G. Schubert, and P. C. Thomas, "Shape, Mean Radius, Gravity Field, and Interior Structure of Callisto," *Icarus*, No. 153, 2001.

[17] J. D. Anderson, E. L. Lau, W. L. Sjogren, G. Schubert, and W. B. Moore, "Gravitational Constraints on the Internal Structure of Ganymede," *Nature*, No. 384, December 1996, pp. 541–543.

[18] J. D. Anderson, G. Schubert, R. A. Jacobson, E. L. Lau, W. B. Moore, and W. L. Sjogren, "Europa's Differentiated Internal Structure: Inferences from Four Galileo Encounters," *Science*, No. 281, 1998.

[19] J. D. Anderson, R. A. Jacobson, E. L. Lau, W. B. Moore, and G. Schubert, "Io's Gravity Field and interior Structure," *Journal of Geophysical Research*, No. 106, 2001.

[20] A. E. Lynam, "Broad-Search Algorithms for Finding Triple- and Quadruple-Satellite-Aided Captures at Jupiter from 2020 to 2080," *Celestial Mechanics and Dynamical Astronomy*, Vol. 121, 2015.

[21] A. E. Lynam, K. W. Kloster, and J. M. Longuski, "Multiple-satellite-aided Capture Trajectories at Jupiter using the Laplace Resonance," *Celestial Mechanics and Dynamical Astronomy*, Vol. 109, No. 1, 2011.

[22] A. E. Lynam and J. M. Longuski, "Interplanetary Trajectories for Multiple Satellite-Aided Capture at Jupiter," *Journal of Guidance, Control, and Dynamics*, Vol. 34, No. 5, September-October 2011.

[23] A. E. Lynam, "Broad-search Algorithms for the Spacecraft Trajectory Design of Callisto-Ganymede-Io triple flybys from 2024-2040, Part I: Heuristic Pruning of the Solution Space," *Acta Astronautica*, Vol. 94, 2014.

[24] A. E. Lynam, "Broad-search Algorithms for the Spacecraft Trajectory Design of Callisto-Ganymede-Io triple flybys from 2024-2040, Part II: Lambert Pathfinding and Trajectory Solutions," *Acta Astronautica*, Vol. 94, 2014.

[25] A. M. Didion and A. E. Lynam, "Impulsive Trajectories from Earth to Callisto-Io-Ganymede Triple Flyby Capture at Jupiter," *Journal of Spacecraft and Rockets*, Vol. 52, 2015.

[26] S. K. Patrick and A. E. Lynam, "Optimal SEP Trajectories from Earth to Jupiter with Triple Flyby Capture," *AIAA Paper No: 2014-4218, AIAA/AAS Astrodynamics Specialist Conference*, San Diego, CA, August 2014.

[27] M. Schadegg, R. P. Russell, and G. Lantoine, "Jovian Orbit Capture and Eccentricity Reduction Using Electrodynamic Tether Propulsion," *Journal of Spacecraft and Rockets*, Vol. 52, 2015.

[28] S. K. Patrick and A. E. Lynam, "High-fidelity Low-thrust SEP trajectories from Earth to Jupiter Capture," *AAS Paper No 15-609, AAS/AIAA Astrodynamics Specialist Conference*, Vail, CO, August 2015.

[29] A. M. Didion and A. E. Lynam, "Guidance and Navigation of a Callisto-Io-Ganymede Triple Flyby Jovian Capture," *AAS Paper No 15-624, AAS/AIAA Astrodynamics Specialist Conference*, Vail, CO, August 2015.

[30] J. R. Johannesen and L. A. D'Amario, "Europa Orbiter Mission Trajectory Design," *AAS Paper 99-330, Proceedings of the AAS/AIAA Astrodynamics Conference*, Vol. 103, Girdwood, AK, August 1999.

[31] D. Landau, N. Strange, and T. Lam, "Solar Electric Propulsion with Satellite Flyby for Jovian Capture," *Proceedings of the AAS/AIAA Spaceflight Mechanics Conference*, San Diego, CA, February 2010.

[32] N. Strange, D. Landau, R. Hofer, J. Snyder, T. Randolph, S. Campagnola, J. Szabo, and B. Pote, "Solar Electric Propulsion Gravity-Assist Tours For Jupiter Missions," *AIAA Paper No: 2012-4518, Proceedings of the AIAA/AAS Astrodynamics Specialists Conference*, Minneapolis, MN, August 2012.

[33] D. Izzo, L. F. Simões, M. Märtens, G. C. H. E. d. Croon, A. Heritier, and C. H. Yam, "Search for a Grand Tour of the Jupiter Galilean Moons," *Proceedings of the 15th Annual Conference on Genetic and Evolutionary Computation*, Amsterdam, The Netherlands, July 2013.

[34] A. E. Lynam, "Broad Search for Trajectories from Earth to Callisto-Ganymede-JOI Double-satellite-aided Capture at Jupiter from 2020 to 2060," *Celestial Mechanics and Dynamical Astronomy*, 2015.

[35] A. Lynam and A. Didion, "Navigation and Statistical Delta-v Analysis for Double-satellite-aided Capture at Jupiter," *AAS Paper No 16-228, AAS/AIAA Spaceflight Mechanics Meeting*, Napa Valley, CA, February 2016.

[36] E. Lancaster and R. Blanchard, "A Unified Form of Lambert's Theorem," tech. rep., NASA technical note TN D-5368, 1969.

[37] R. Gooding, "A Procedure for the Solution of Lambert's Orbital Boundary-Value Problem," *Celestial Mechanics and Dynamical Astronomy*, Vol. 48, 1990.

[38] B. Donahue and D. Sauvageau, "The Space Launch System Capabilities for Beyond Earth Missions," *Paris SLS missions*, Paris, France, April 2014.

[39] S. Hughes, "GMAT-Generalized Mission Analysis Tool," tech. rep., NASA Goddard Space Flight Center, Greenbelt, MD, 2008.

[40] T. Lam, J. J. Arrieta-Camacho, and B. B. Buffington, "The Europa Mission: Multiple Europa Flyby Trajectory Design Trades and Challenges," *AAS Paper No 15-657, AAS/AIAA Astrodynamics Specialist Conference*, Vail, CO, August 2015.

[41] P. Goldreich, "An Explanation of the Frequent Occurrence of Commensurable Mean Motions in the Solar System," *Journal of the Royal Astronomical Society*, Vol. 130, 1965.

[42] K. Kloster, A. Petropoulos, and J. Longuski, "Europa Orbiter Tour Design with Io Gravity Assists," *Acta Astronautica*, Vol. 68, 2010, pp. 931–946.